DEFORMATION BEHAVIOR OF THIN

LUBRICANT FILMS AT ELEVATED PRESSURE -

VISCOMETRIC FUNCTIONS

Annual Report to

Office of Naval Research
800 North Quincy Street
Arlington, VA 22217-5000

Scott Bair
Principal Research Engineer
Woodruff School of Mechanical Engineering
Georgia Institute of Technology

January 1996

Summary

Although normal stress differences in liquids have conventionally been associated with polymers, aspects of rheological behavior in lubricated concentrated contacts suggest that normal stress difference may be significant in even low molecular weight liquids sheared under high pressure and high shear stress. A torsional flow rheogoniometer was constructed for use at high (300 MPa) pressure. Four typical liquid lubricants were investigated, including one polymer/mineral oil solution. Shear stress and N_1 - N_2 are reported as functions of shear rate. The effect of pressure variation is reported for two liquids. Results are compared with predictive techniques and a molecular dynamics simulation. Simple low molecular weight lubricant base oils can generate measurable and significant normal stress differences when sheared at high shear stress.

Introduction

Viscoelasticity in liquids has conventionally been associated with high polymers. The related phenomena of shear-thinning and normal stress differences in simple shear are not ordinarily associated with simple low-molecular weight liquids. The exception would be the lubrication of concentrated contacts with typical liquid lubricants. The assumption of Newtonian behavior for the lubricant film nearly always leads to large errors in the prediction of traction (friction). Early models of elastohydrodynamic lubricant rheology invoked viscoelasticity (Dyson, 1970 and Chow and Saibel, 1971), the assumption being that the high-pressure of the film sufficiently raised the glass transition temperature of the liquid to make elasticity important. The shear-thinning aspect brought theory into agreement with experiment. Shear-thinning models have been refined to the extent that for some cases, traction curves can be accurately calculated from flow curves obtained with rheometers at high-pressure (Bair, 1994). The second consequence of viscoelastic response, the normal stress difference, has been neglected in studies of concentrated contact lubrication - possibly because Tanner (1967) argued that to affect the load capacity of a lubricant film, the ratio of the first normal stress difference to the shear stress must be significant when compared with the length to thickness ratio of the film. His argument was not fully accepted at the time.

Recent developments have motivated a fresh look at normal stresses in liquids under pressure. Polymer solutions in concentrated contact have been found to build films significantly thicker than would be expected from the shear viscosity of the solution when the films are very thin (Cann and Spikes, 1994). The first normal stress difference acts to augment the load

carrying capacity of a liquid in shear and polymer solutions are well known to generate a large first normal stress difference. Normal stresses have been obtained for molecularly thin liquid films sheared between atomistically smooth boundaries (Reiten, et al., 1994). A non-equilibrium molecular dynamics simulation of a liquid lubricant sheared at high-pressure has predicted (Berker, et al., 1992) a first normal stress difference which exceeds the shear stress. The orientation of shear bands which are observed in liquids under pressure and high shear stress (Bair, et al., 1993) can so far only be explained by a first normal stress difference which is comparable to the shear stress (Bair and Winer, 1993a). Normal stress differences may be necessary to provide the geometric instability which precipitates slip along shear bands (Lee, et al., 1994) in liquid lubricants.

Background

The experimental flows, which are used to measure the viscometric functions of liquids, reduce at least at some small scale to a steady simple shearing which is shown in Figure 1. Flow is in direction 1 with the velocity gradient in direction 2. The shear rate, $\dot{\gamma}$, is the magnitude of the velocity gradient and is twice the non-zero component of the deformation rate tensor, d_{12}. From symmetry the only non-zero shear stress is $\tau = \sigma_{12} = \sigma_{21}$ and must be an odd function of $\dot{\gamma}$. The mean mechanical pressure is $p = -(\sigma_{11} + \sigma_{22} + \sigma_{33})/3$ and is not set by these flow kinematics. Only the differences between normal stresses can be determined from the flow and it is known from symmetry that they must be even functions of shear rate. The first normal stress difference, N_1, is as shown in Figure 1, the difference between the normal stresses in the flow direction and in the velocity gradient direction. The second normal stress difference is the

difference between the normal stresses in the velocity gradient direction and the neutral direction. We have

$$\tau = \sigma_{12} = \eta(\dot{\gamma})\dot{\gamma} \tag{1}$$

$$N_1 = \sigma_{11} - \sigma_{22} = \psi_1(\dot{\gamma})\dot{\gamma}^2 \tag{2}$$

$$N_2 = \sigma_{22} - \sigma_{33} = \psi_2(\dot{\gamma})\dot{\gamma}^2 \tag{3}$$

where η is the coefficient of apparent (or effective) viscosity and ψ_1 and ψ_2 are the first and second normal stress coefficients respectively.

The large body of experience obtained with polymeric liquids tells us that all three coefficients (the viscometric functions) are monotonically decreasing in $\dot{\gamma}$ and

$$\eta(\dot{\gamma} \to 0) = \eta_0 = \mu \tag{4}$$

$$\psi_1(\dot{\gamma} \to 0) = \psi_{10} \tag{5}$$

$$\psi_2(\dot{\gamma} \to 0) = \psi_{20} \tag{6}$$

in the terminal regime. In general N_1 is positive, N_2 is negative and $|N_2| << |N_1|$. We will make use of the latter at times to justify use of the Weissenberg hypothesis that $N_2 = 0$.

The constitutive equation for a Newtonian liquid is

$$\sigma_{ij} = -\delta_{ij} p_T + 2\mu d_{ij} + \mu_s \delta_{ij} d_{kk} \tag{7}$$

where p_T is the thermodynamic pressure and μ_s is the second coefficient of viscosity. Then for a Newtonian liquid $\eta \equiv \mu$, $N_1 \equiv 0$ and $N_2 \equiv 0$. Notice that the thermodynamic pressure which is obtained from an equilibrium equation of state is not necessarily equal to p. Indeed, for compressible viscoelastic liquids with normal stress differences, a precise definition of pressure is beyond current understanding (Ko and Bogue, 1987).

The Mohr-Coulomb criterion is useful for describing the orientation of shear bands in a simple shear experiment (Bair and Winer, 1993a). Slip will occur on a plane for which the shear stress has reached a critical value which follows a linear variation with the compressive normal stress on the slip plane. At high-pressure the critical stress becomes nearly proportional to pressure with the portionality constant being an internal friction coefficient which is a material property. Three idealizations of liquid response are shown in Figure 2 along with the resulting shear bands. The horizontal lines are solid boundaries to a liquid film. The lower boundary is stationary and the upper boundary moves with velocity, v. The top case shown in Figure 2a is for a pressure insensitive liquid (internal friction coefficient = 0) with zero first normal stress difference, N_1. The shear bands are aligned with the principal shear strain rate axes as shown. The second case (Figure 2b) is for a pressure sensitive liquid and $N_1 = 0$. The shear bands are rotated off of the principal shear directions in a sense which will reduce the compressive normal stress on the planes of the shear bands. In Figure 2c the pressure sensitive liquid has an extra tensile stress in the flow direction, i.e., $N_1 > 0$. Effectively, the principal shear stress axes and the shear bands have been rotated from the principal shear strain rate axes in the direction of material rotation. Comparison with the micrograph of shear bands (Figure 2d) shows that the complete description requires both pressure sensitivity and $N_1 > 0$.

Instruments

The rheometers used in this study were of two types. Measurements of shear stress as a function of shear rate in Couette flow were performed with a High-Pressure High-Shear Stress Viscometer which was described in detail elsewhere (Bair and Winer, 1993b). Measurements of

both shear stress and normal stress difference in torsional flow were obtained with a new High-Pressure Rheogoniometer. This instrument was constructed by replacing the concentric cylinder pair, torque transducer and closure in the pressure vessel of the Couette device by a rheogoniometer cartridge which is shown in Figure 3. In the High-Pressure Rheogoniometer the pressurized sample liquid occupies the entire space around the cartridge. The liquid sample is sheared in the gap between parallel planes formed by the end of a rotating spindle shaft above and a fixed cap below. The radius, R, of the shear gap is 2.39 mm. The spindle shaft is made of high-thermal conductivity, high-strength W-Cu composite and is supported by two ball bearings with low viscosity diester lubricant sealed within a housing shown at the top of Figure 3. The cap was constructed of W-Cu composite and attached through a non-rotating ball and socket joint to a two channel dynamometer. This dynamometer provides measurement of torque, Q, and thrust force, F, on the cap. It consists of an aluminum cylindrical shell of 0.1 mm thickness with two full strain gauge bridges applied. The dynamometer is coupled to the spindle housing through a spring preloaded compound screw which provides adjustment of the gap, h, by 25 μm per screw revolution. The strain gauge signals are passed through the closure plug by six electrodes. The counter surfaces of the shear gap were lapped against one another with diamond paste until the contact patch was uniform.

Torsional flow between rotating parallel planes provides measurements of viscometric functions which are free of the controversy associated with some other techniques. The calibration relations have been derived many times and can be found in most rheology texts. They are written for conditions at the gap edge (maximum shear rate, $\dot{\gamma} = \Omega R / h$) as

$$\tau = \frac{3Q}{2\pi R^3}\left[1 + \frac{1}{3}\frac{d\log Q}{d\log\Omega}\right] \tag{8}$$

$$N_1 - N_2 = \frac{2F}{\pi R^2}\left[1 + \frac{1}{2}\frac{d\log F}{d\log\Omega}\right] \tag{9}$$

where Ω is rotating rate in radians/s. The derivatives in the brackets provide a correction for the nonuniformity of shear rate. Note that the normal stress difference which is measured is $N_1 - N_2$. If the magnitude of N_2 is small compared to N_1, then this measurement can be compared to N_1 without significant error.

The thrust force, F, is due to a directly acting normal stress superimposed on a pressure profile which increases with decreasing radius along the shear gap. The normal stress differences produce a tensile hoop stress which generates the radial pressure profile. The pressure which we directly measured (with a gauge) is the pressure of the liquid surrounding the shear gap, p_s. The boundary condition at the edge of the gap is $p_s = -\sigma_{33}$. From the definitions of mean mechanical pressure and normal stress differences, at the edge $p = p_s - (N_1 + 2N_2)/3$. A precise knowledge of experimental pressure would require separate measurement of N_1 and N_2. In this study $(N_1 - N_2)/3$ was never greater than 2% of p_s so we will approximate $p \approx p_s$.

The dynamometer was designed to provide similar sensitivity to $N_1 - N_2$ and τ in terms of signal volts per unit stress. Cross-talk was found to be less than 3%.

Experiment

Four liquids which have been used as concentrated contact lubricants were the subject of this study. Three of the liquids are base oils and these are some of the most thoroughly characterized (Bair, 1994 and references therein) liquids in the tribology literature. They are 143

AD - perfluoropolyalkylether, LVI 260 - mineral oil, and 5P4E - polyphenyl ether. A polymer blend, LF 5346, was also included, because polymer solutions are well known to display normal stress differences at atmospheric pressure and they are an important class of lubricants. The polymer is polybutene with number average molecular weight of 25,000 and weight average molecular weight of 50,000 and is blended with 80 percent mineral oil with kinematic viscosity of 18 mm^2/s at 38°C.

The operation of the Couette flow device has been described previously (Bair and Winer, 1993b). For the High-Pressure Rheogoniometer, the shear gap, h, was determined by generating flow curves in both Couette and torsional flow on the same material at the same pressure and temperature and shifting the torsional flow data by varying h until they superimposed.

Viscous heating is reduced by maintaining h as small as possible. Experiments in torsional flow with h as small as 2 μm gave poor repeatability, possibly due to significant relative changes in the gap, h, with normal force because of the compliance of the dynamometer. A gap of 9.7 μm was used for all reported results as a good compromise between viscous heating and repeatability. For this value of h and a typical temperature viscosity coefficient and liquid thermal conductivity, viscous heating will be significant for a dissipation of $\tau\dot{\gamma} = 10^{10}\ W/m^3$. This corresponds to a Brinkman number of one. The Couette flow measurements were performed with a gap of 1.2 μm and a significantly higher viscous heating limit of about $\tau\dot{\gamma} = 2 \times 10^{11}\ W/m^3$.

A typical thrust/torque history is shown in Figure 4. At start-up the rotational velocity was increased linearly with time until the test velocity was reached at 50 ms. Note that the torque measurement response is much faster than the thrust measurement response. This is the

"squeeze damping effect" which results from the small increase of the gap in response to the thrust force and the retardation of flow into the gap by the very large viscosity of the liquid. When the direction of rotation was reversed, the thrust was unchanged and the torque changed sign as expected.

Results

Flow curves for the four liquid lubricants are shown in Figures 5-8 at indicated pressure where the closed circles represent shear stress measured in Couette flow and all other data points are for torsional flow. All tests were at 20°C. These are apparently the first measurement of normal stress in liquids under high-pressure. For the three base oils; 143 AD, LVI 260, and 5P4E the normal stress difference, $N_1 - N_2$ was always less than the shear stress, τ. For the polymer solution the normal stress difference was always greater than the shear stress for the rates of shear investigated. Note that for LF 5346, $N_1 - N_2$ attained a value of 12 MPa which may be the highest experimentally measured normal stress difference for a liquid.

Viscous heating effects can clearly be seen for the torsional flow (open circles) in Figures 5 and 6 where the shear stress becomes less than that measured in the Couette device for $\tau\dot{\gamma} > 10^{10}\ W/m^3$.

Discussion

Methods for obtaining engineering estimates of the first normal stress difference when the viscosity function is known are available in the rheology literature (Dekee and Stastna, 1986).

Two are listed here. The first is due to Abdel-Khalik, et al. (1974) and was derived from a rheological equation of state.

$$\psi_1(\dot{\gamma}) = \frac{4\kappa}{\pi}\int_0^{\infty}\frac{\eta(\dot{\gamma}) - \eta(s)}{s^2 - \dot{\gamma}^2}ds \tag{10}$$

$$2 \le \kappa \le 3$$

The second is due to Gleissle (1982) and follows from empirical rules.

$$\psi_1(\dot{\gamma}) = 2\int_{\eta(\infty)}^{\eta(\dot{\gamma}/\kappa)}\frac{d\eta}{\dot{\gamma}} \tag{11}$$

$$2 \le \kappa \le 3$$

A recursion formula for approximation of (11) was also given.

$$\psi_1(\kappa(\dot{\gamma} - \Delta\dot{\gamma})) = \psi_1(\kappa\dot{\gamma}) - \frac{2[\eta(\dot{\gamma}) - \eta(\dot{\gamma} - \Delta\dot{\gamma})]}{\sqrt{(\dot{\gamma} - \Delta\dot{\gamma})\dot{\gamma}}} \tag{12}$$

Note that the dimensionless shifting parameter κ has a different meaning in equations (10) and (11) although the stated range is the same. In the former, κ shifts ψ_1 and in the latter κ shifts $\dot{\gamma}$.

The line plotted through the shear stress data in Figure 8 represents the power law for a power law exponent of N = 0.35.

$$\eta = A\dot{\gamma}^{-N} \tag{13}$$

Equation (10) combined with the power law (13) was solved by Abdel-Khalik (1974) and is shown in Figure 8 for $\kappa = 3$. Inserting the power law (13) into equation (11) results in

$$\psi_1(\dot{\gamma}) = \frac{2N}{1+N}A\kappa^{1+N}\dot{\gamma}^{-(1+N)} \tag{14}$$

which is plotted as Gleissle in Figure 8 for $\kappa = 3$. These predictions bracket our measurements of N_1 - N_2 for the polymer solution.

It is of interest to apply these engineering predictions to low molecular weight liquids which have not previously been considered in tests of these predictions. The viscosity function, η, is plotted against shear rate in Figures 9-11 for the base oils. Again, solid circles are Couette flow. For shear rates which are greater than the experimental capability, equation (14) was applied and for shear rates at which η has been measured the recursion formula (12) was used to give the predicted first normal stress coefficient, ψ_1 plotted in Figures 9-11. The values of κ required to obtain the fit to the experimental data are shown in the figures. Remember, the data points plotted for comparison are $(N_1 - N_2)/\dot{\gamma}^2$ or $\psi_1 - \psi_2$.

We know, however, that the measurements of viscosity shown in the figures do not represent constitutive behavior for rates greater than the rate at which the first shear bands appear (Bair and Winer, 1993). A portion of the velocity used in the calculation of the velocity gradient in these measurements was contributed by slip along the shear bands. Therefore, as a check, in Figure 10 for the mineral oil, it was assumed that the constitutive behavior followed a power law above the arbitrary shear rate of 250 s^{-1} as shown by the broken line. The prediction for ψ_1 is nearly the same for the two approaches within the experimental range of measurement of ψ_1 - ψ_2 and we can conclude that localization in Couette flow does not affect our comparisons - only the extrapolations.

For polymers, κ varies from 2 to 3; however, for the low molecular weight base oils investigated we found a value of 0.4 to 1 to be more appropriate. This may be the result of a difference in molecular mechanism for normal stresses for the different materials. The non-linear stretching of entangled molecules will not enhance the extra tensile stress in the flow direction for the low molecular weight base oils.

The relationship between N_1 (or N_2) and τ has been found to be a characteristic of a particular polymer (eg. Tanner, 1973). Han and Jhon (1986) showed that N_1 vs. $\dot{\gamma}$ isotherms for various temperatures could be shifted to superimpose upon a master curve by plotting N_1 vs. τ. Tanner (1985) showed that the relation between N_1 and τ should be a weak function of temperature by time-temperature superposition. We know that time-temperature shifting can be generalized to include pressure as well as temperature so that the relation between N_1 and τ should also be insensitive to pressure. We have plotted $N_1 - N_2$ versus τ in Figure 12 for LF 5346 and 5P4E. Also included are results at reduced pressure as represented by the solid data points. The shear rates for these reduced pressures were four and ten times greater for the same shear stress for LF 5346 and 5P4E respectively because the low shear viscosity, μ, was reduced by this ratio. However, the relationship between $N_1 - N_2$ and τ as shown in the figure is little changed by pressure.

Continuum models predict that in the terminal regime (Larson, 1988)

$$N_1(\dot{\gamma} \to 0) = \frac{2}{G}\tau^2 \tag{15}$$

The Rouse molecular model gives (Larson, 1988) for the modulus, $G = nkT$ so that

$$N_1(\dot{\gamma} \to 0) = \frac{2}{nkT}\tau^2 \tag{16}$$

where k is the Boltzmann constant, T is absolute temperature and n is the number of polymer molecules per unit volume. Equation (16) is plotted for the polymer blend, LF 5346, in Figure 12 assuming $N_2 = 0$. The molecular volume of 5P4E (molecular weight, 450) was used to calculate n and the result is also plotted. Both results (the solid lines in Figure 12) may adequately represent the low shear stress behavior of these liquids. The value of G for 5P4E, 6

MPa, is two orders of magnitude lower than the limiting high frequency shear modulus, G_∞, which has been measured by various techniques (Bair, 1994). G should be the modulus associated with the longest relaxation time.

The orientation of shear bands in simple shear was noted for 5P4E and the ratio of first normal stress to shear stress was calculated from Mohr-Coulomb theory to be 1.26 (Bair and Winer, 1993a). The shear stress was approximately 20 MPa. The broken line in Figure 12 is $N_1 = 1.26\ \tau$ assuming $N_2 = 0$. Extrapolation of terminal behavior would reach the predicted ratio well in advance of 20 MPa shear stress; however the experimental measurements show a trend which falls short of the predicted ratio of N_1 to τ. The calculation of $\psi_1(\dot{\gamma})$ for 5P4E in Figure 11 by equation (11) for $\kappa = 1$ gives the result that $N_1/\tau \to 1$ at high-shear stress. If $\kappa = 1.12$ instead, the ratio of N_1 to τ required by the shear band orientation is obtained.

Berker and coworkers (1992) have performed a non-equilibrium molecular dynamic (NEMD) simulation of a lubricant under concentrated contact conditions. The model lubricant was the hydrocarbon, n-hexadecane, at high-pressure and high-temperature. The simulation allowed chemical bonds to stretch and bend. Homogeneous constant volume shear was imposed and the viscometric functions were reported over a large range of shear rate. The constant volume constraint caused the mean mechanical pressure to increase with shear rate (and shear stress). However, we have shown above that a presentation of normal stress difference versus shear stress removes or reduces the pressure effect. The results of Berker, et al. (1992) are plotted in Figure 13. At the lowest shear rate (and lowest shear stress) a large uncertainty was reported as shown in the figure. The present experimental results for the hydrocarbon, LVI 260, are plotted in the same figure and are consistent with the NEMD results. The molecular weight

of LVI 260 is 425; about twice that of hexadecane. The terminal normal stress difference according to equation (16) should be proportional to molecular weight for equal density. Halving the measured normal stress difference for LVI 260 would place the results in the center of the results of the NEMD simulation.

Normal stress differences have not been measured for low molecular weight base oils at atmospheric pressure by conventional rheogoniometers. The reason for this is apparent from equation (16). If the smallest measurable N_1 is 10 Pa, the shear stress, τ, must be at least 5000 Pa. This shear stress is difficult to reach with a relatively low viscosity (~1 Pa·s) liquid in a conventional rheometer without significant viscous heating. Also, for low viscosity, inertia effects dominate over the normal stress for conventional measurement techniques. High-pressure is helpful in that the viscosity can be very large.

Conclusions

1) A High-Pressure Rheogoniometer has been constructed which is capable of measuring shear stress, τ, and the normal stress difference, $N_1 - N_2$ to pressures of 240 MPa and shear rates of at least 10^4 s^{-1}.
2) Simple low molecular weight liquids generate measurable and significant normal stress differences when the shear stress is high and the measured values agree with NEMD simulation.
3) Methods for making engineering estimates of first normal stress difference may be useful for lubricant base oils if the shifting parameter, κ, is less than the value used for polymers.
4) The relationship between $N_1 - N_2$ and τ is a weak function of pressure.

5) Measurements of normal stress differences are not entirely inconsistent with shear band observations; however, normal stress measurements obtained at the critical shear stress for slip are needed.

References

Abdel-Khalik, S., Hassager, O. and Bird, R. B. (1974) "Prediction of Melt Elasticity from Viscosity Data," Polym. Engr. Sci. 14, 12, p. 860.

Bair, S., Qureshi, F. and Winer, W. O. (1993) "Observations of Shear Localization in Liquid Lubricants under Pressure," Trans. ASME J. of Tribology, 115, 3 pp. 507-514.

Bair, S. and Winer, W. O. (1993a) "A Rheological Basis for Concentrated Contact Friction," Proc. Leeds-Lyon Symposium on Tribology.

Bair, S. and Winer, W. O. (1993b) "A New High-Pressure High-Shear Stress Viscometer and Results for Lubricants," STLE Trib. Trans., 36, 4 pp. 721-725.

Bair, S. (1994) "Recent Developments in High-Pressure Rheology of Lubricants," Proc. Leeds-Lyon Symposium on Tribology.

Berker, A., Chynowether, S., Klomp, U. C. and Michopoulos, Y. (1992), "NEMD Simulations and the Rheological Properties of Liquid n-Hexadecane," J. Chem. Soc. Faraday Trans. 88, pp. 1791-1825.

Cann, P. M. and Spikes, H. A. (1994) "The Behavior of Polymer Solutions in Concentrated Contact," STLE Trib. Trans. 37, 3, pp. 580-586.

Chow, T. S. and Saibel, E. (1971) "The Elastohydrodynamic Problem with a Viscoelastic Fluid," ASME J. of Lub. Tech. 93, Series F, 1, p. 25.

Dekee, D. and Stastna, J. (1986) "Primary Normal Stress Coefficient Predictions," J. of Rheology 30, 1, pp. 209-212.

Dyson, A. (1970) "Frictional Traction and Lubricant Rheology in Elastohydrodynamic Lubrication," Phil. Trans. Roy. Soc. A266, p. 1.

Gleissle, W. (1982) "Stresses in Polymer Melts at the Beginning of Flow Instabilities," Rheo. Acta 21, p. 485.

Han, C. D. and Jhon, M. S. (1986) "Correlations of the First Normal Stress Difference with Shear Stress and of the Storage Modulus with Loss Modulus for Homopolymers," J. of Appl. Polym. Sci. 32, p. 3832.

Ko, W. C. and Bogue, D. C. (1987) "A Constitutive Equation Including Compressibility Effects," J. of Rheology 31, 6, p. 437.

Larson, R. G. (1988) Constitutive Equations for Polymer Melts and Solutions, Butterworths, Boston p. 26,221.

Lee, Y. K., Ghosh, J., Bair, S. and Winer, W. O. (1994) "Shear Band Analysis for Lubricants Based on a Viscoelastic Plasticity Model," Appl. Mech. Rev. 47, Part 2, pp. 5209-5220.

Reiter, G., Demirel, A. L. and Granick, S. (1994), "From Static to Kinetic Friction in Confined Liquid Films," Science 263, p. 1743.

Tanner, R. I. (1967) Discussion of Tao and Philippoff (1967) published with paper.

Tanner, R. I. (1973) "A Correlation of Normal Stress Data for Polyisobutylene Solutions," Trans. Soc. Rheology 17, 2, p. 365.

Tanner, R. I. (1985) Engineering Rheology, Clarendon Press, Oxford, p. 358.

Tao, F. F. and Philippoff, W. (1967) "Hydrodynamic Behavior of Viscoelastic Liquids in a Simulated Journal Bearing," ASLE Trans. 10, 3, pp. 302-315.

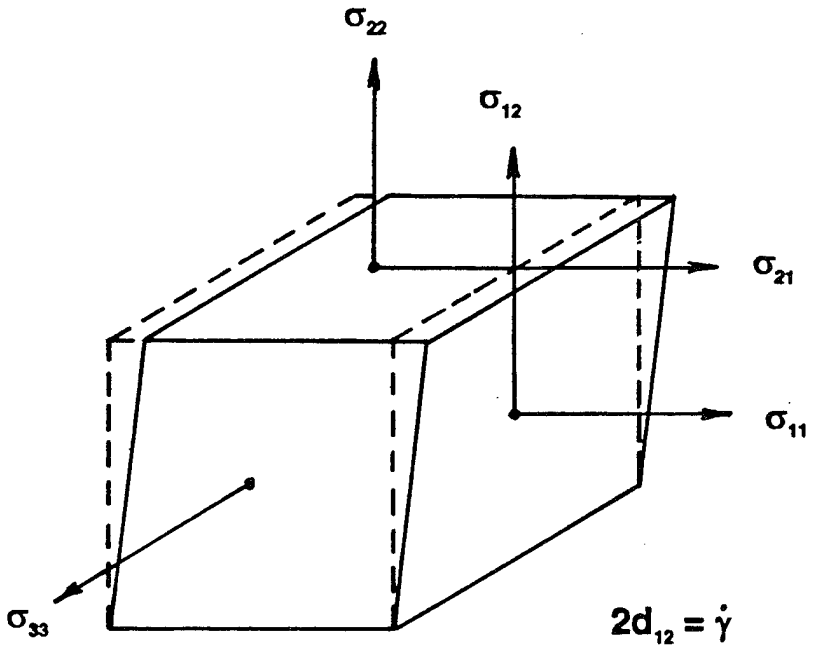

$$\tau = \sigma_{12} = \eta(\dot{\gamma})\,\dot{\gamma}$$
$$N_1 = \sigma_{11} - \sigma_{22} = \psi_1(\dot{\gamma})\,\dot{\gamma}^2$$
$$N_2 = \sigma_{22} - \sigma_{33} = \psi_2(\dot{\gamma})\,\dot{\gamma}^2$$

Figure 1. Definition of Stresses in a Simple Shear Experiment.

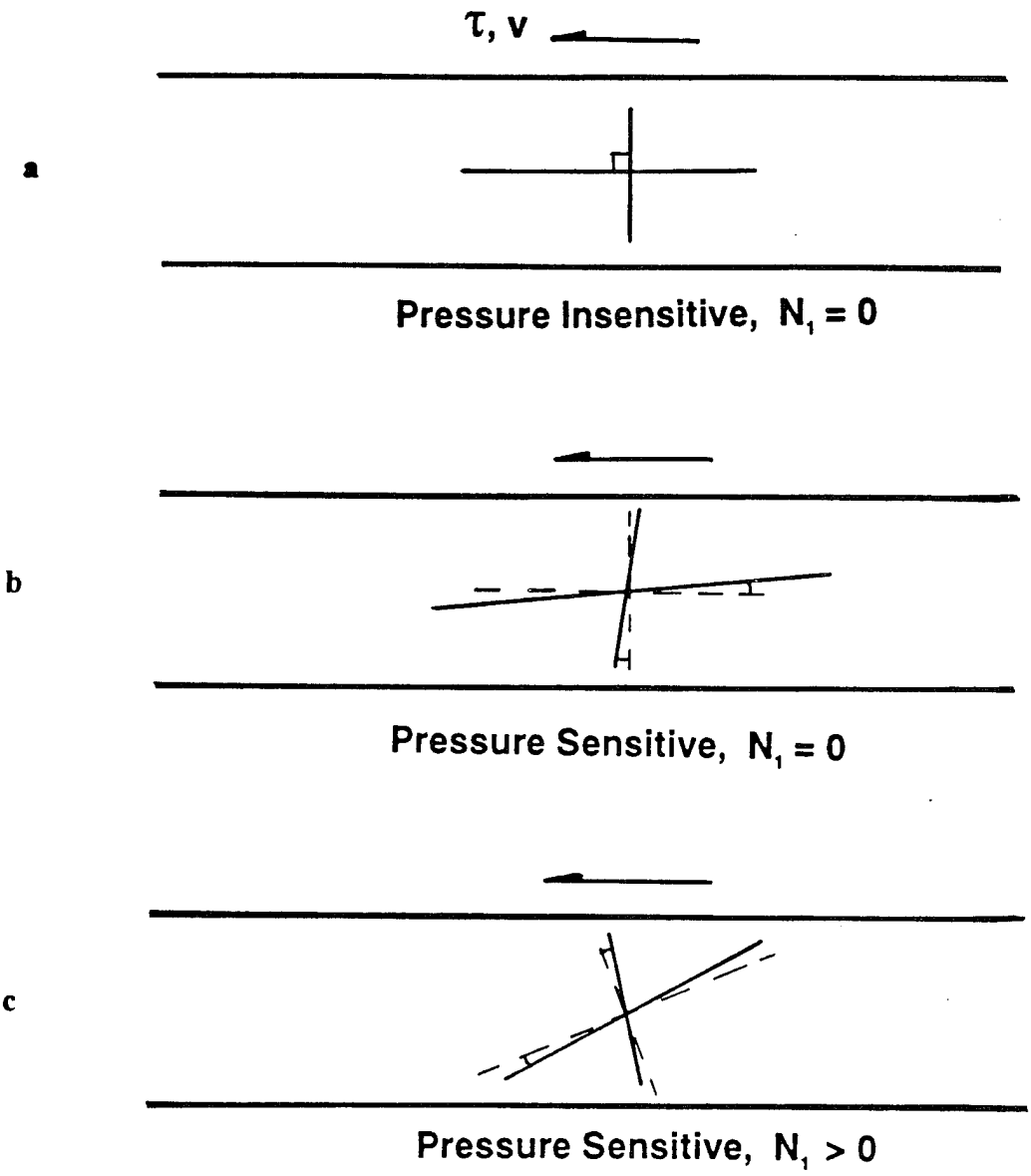

Figure 2. Shear Band Orientation for Mohr Coulomb Theory and Various Idealizations.

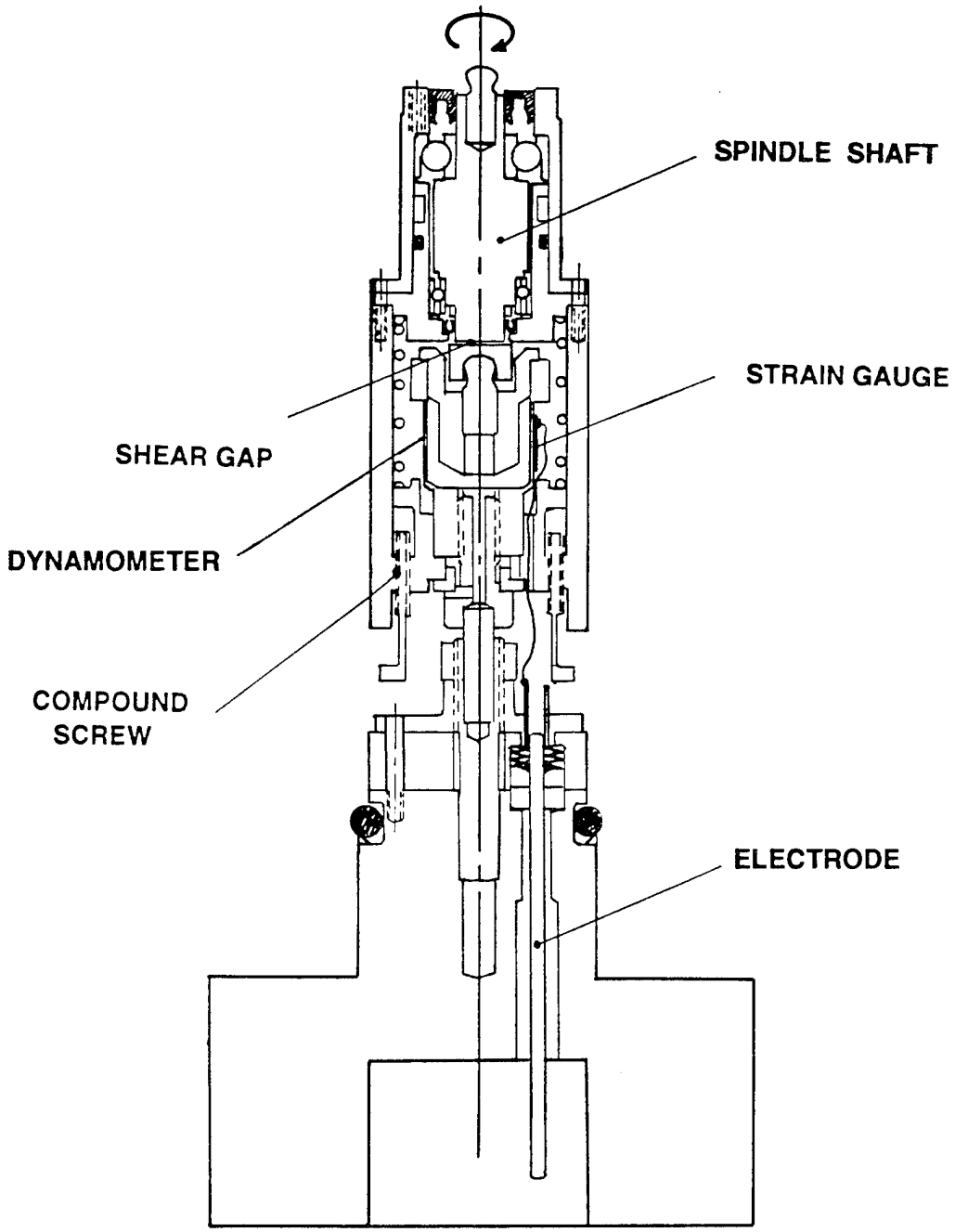

Figure 3. High-Pressure Rheogoniometer Cartridge and Closure.

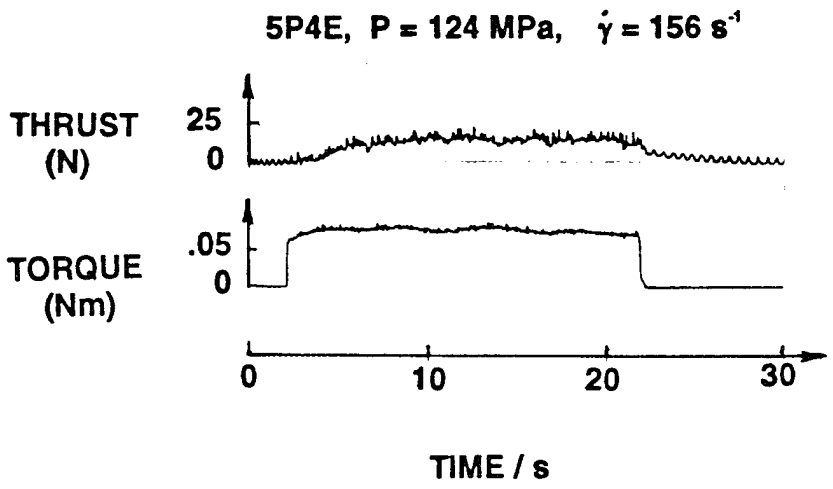

Figure 4. Typical Thrust/Torque Histories for Torsional Flow.

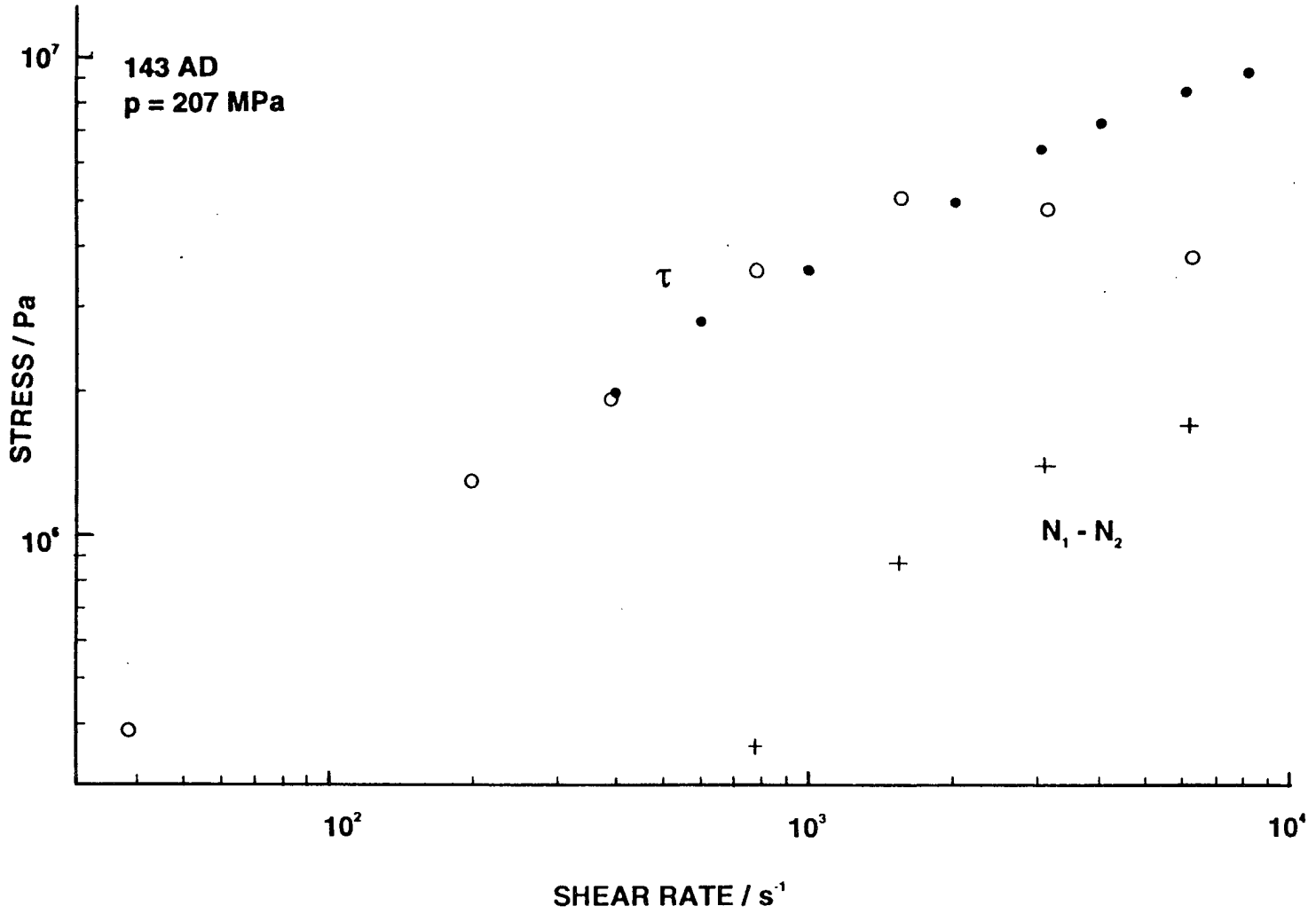

Figure 5. Flow Curves for Perfluoropolyalkylether. Solid Circles from Couette Shear. Others from Torsional Flow.

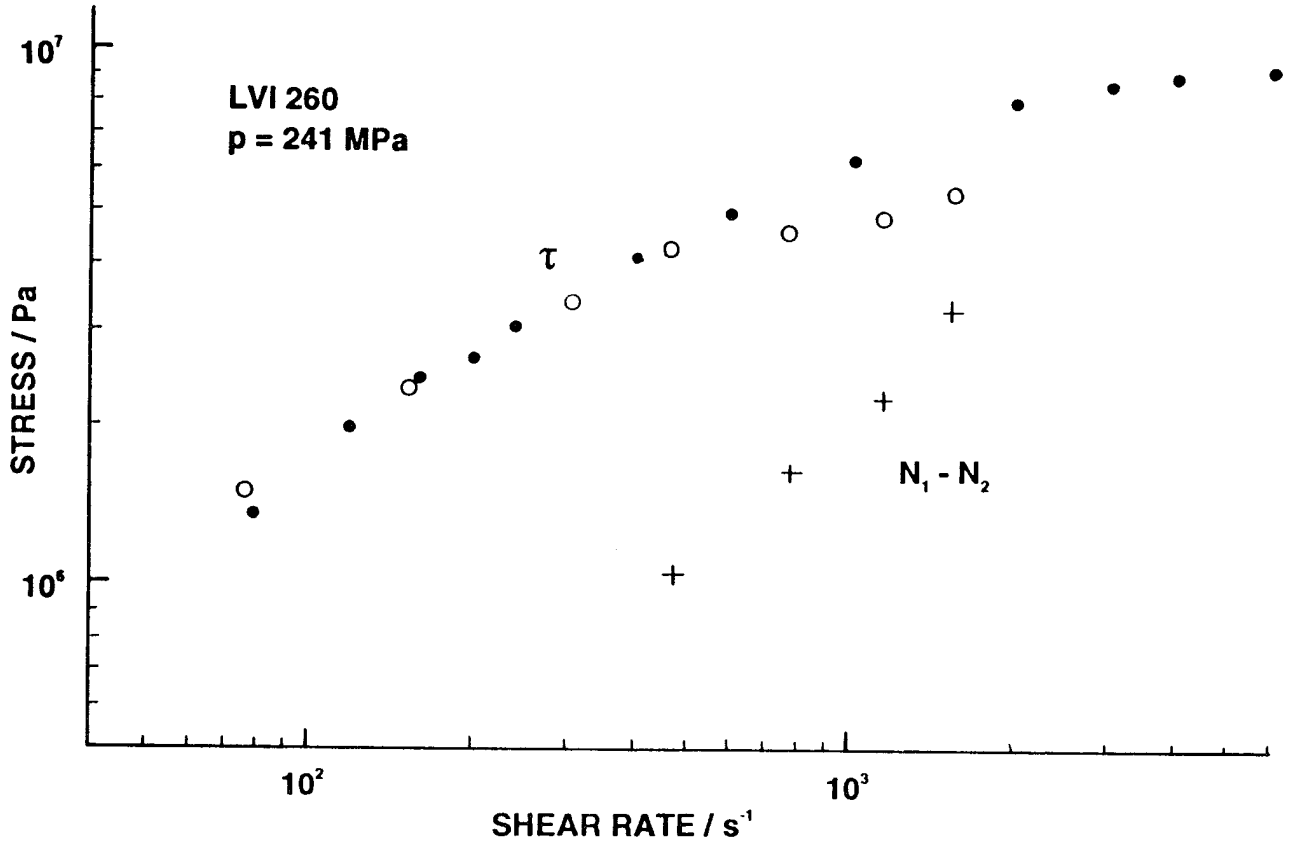

Figure 6. Flow Curves for Mineral Oil. Solid Circles from Couette Shear. Others from Torsional Flow.

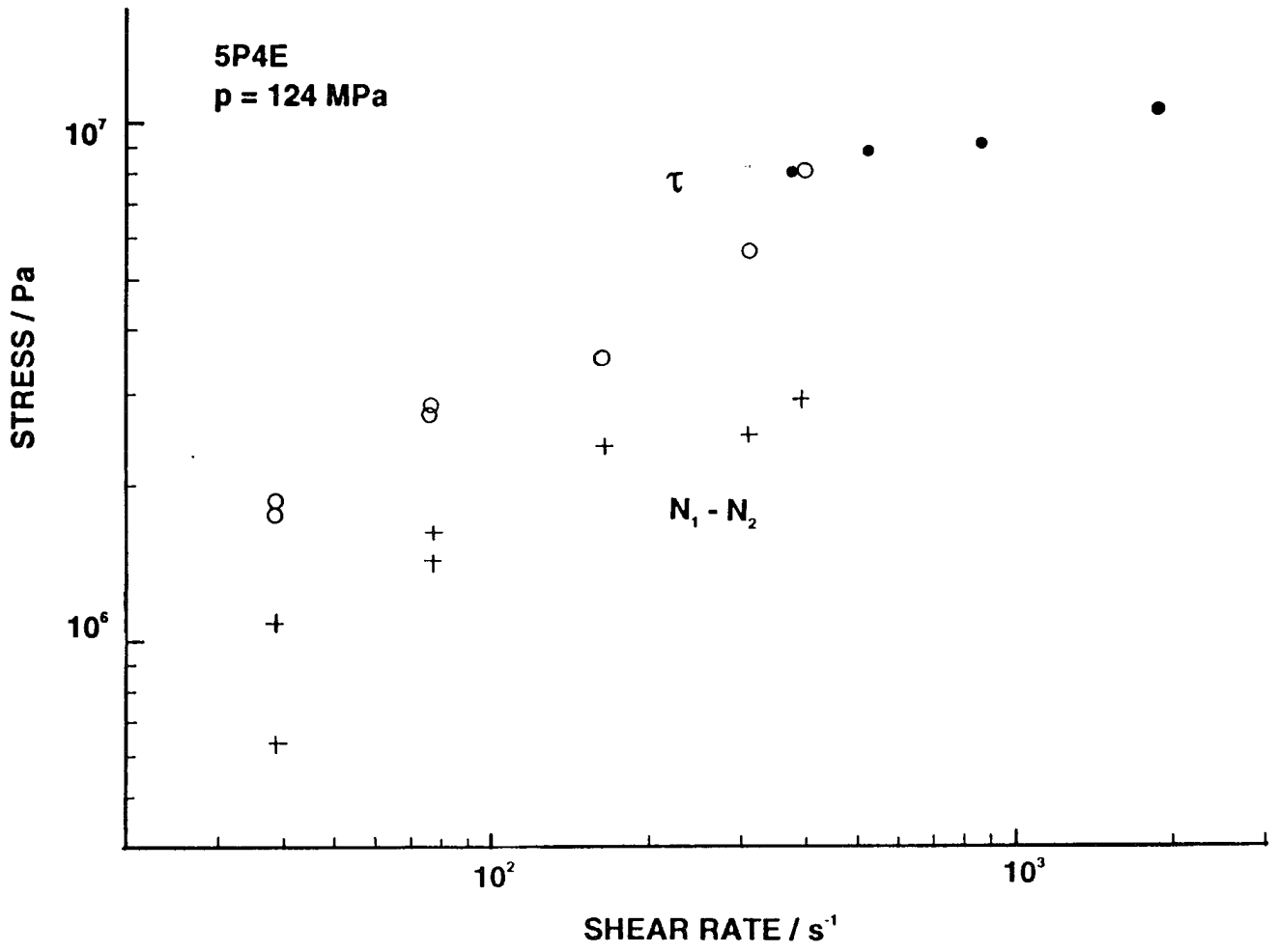

Figure 7. Flow Curves for Polyphenyl ether. Solid Circles from Couette Shear. Others from Torsional Flow.

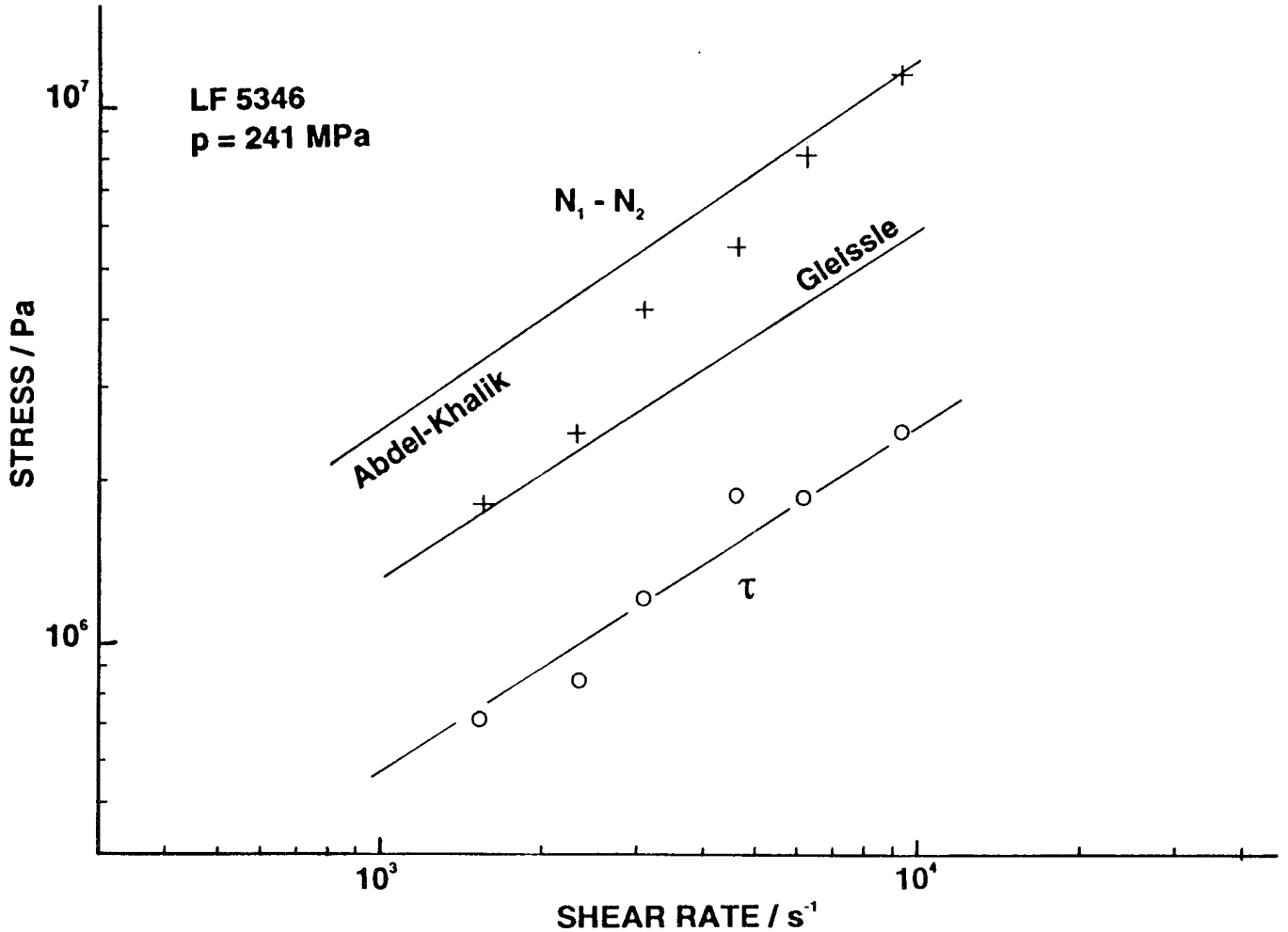

Figure 8. Flow Curves for Polybutene in Mineral Oil. Power Law Fitted to τ. Predictive Methods are shown for $N_1 - N_2$ Using

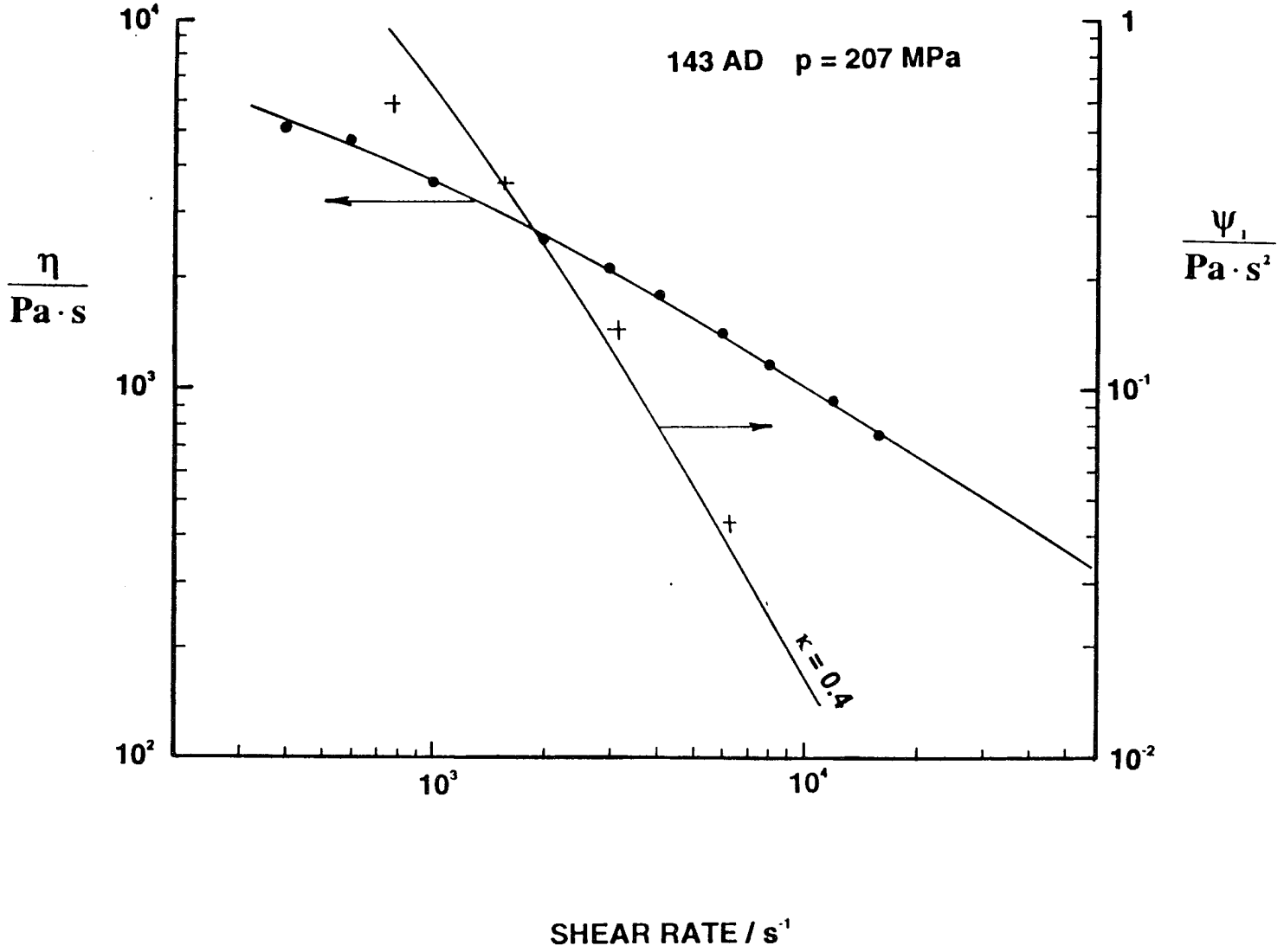

Figure 9. Viscosity and First Normal Stress Coefficient versus Shear Rate for 143 AD. The prediction of Equation (11) is plotted. ψ_1 - ψ_2 plotted as +.

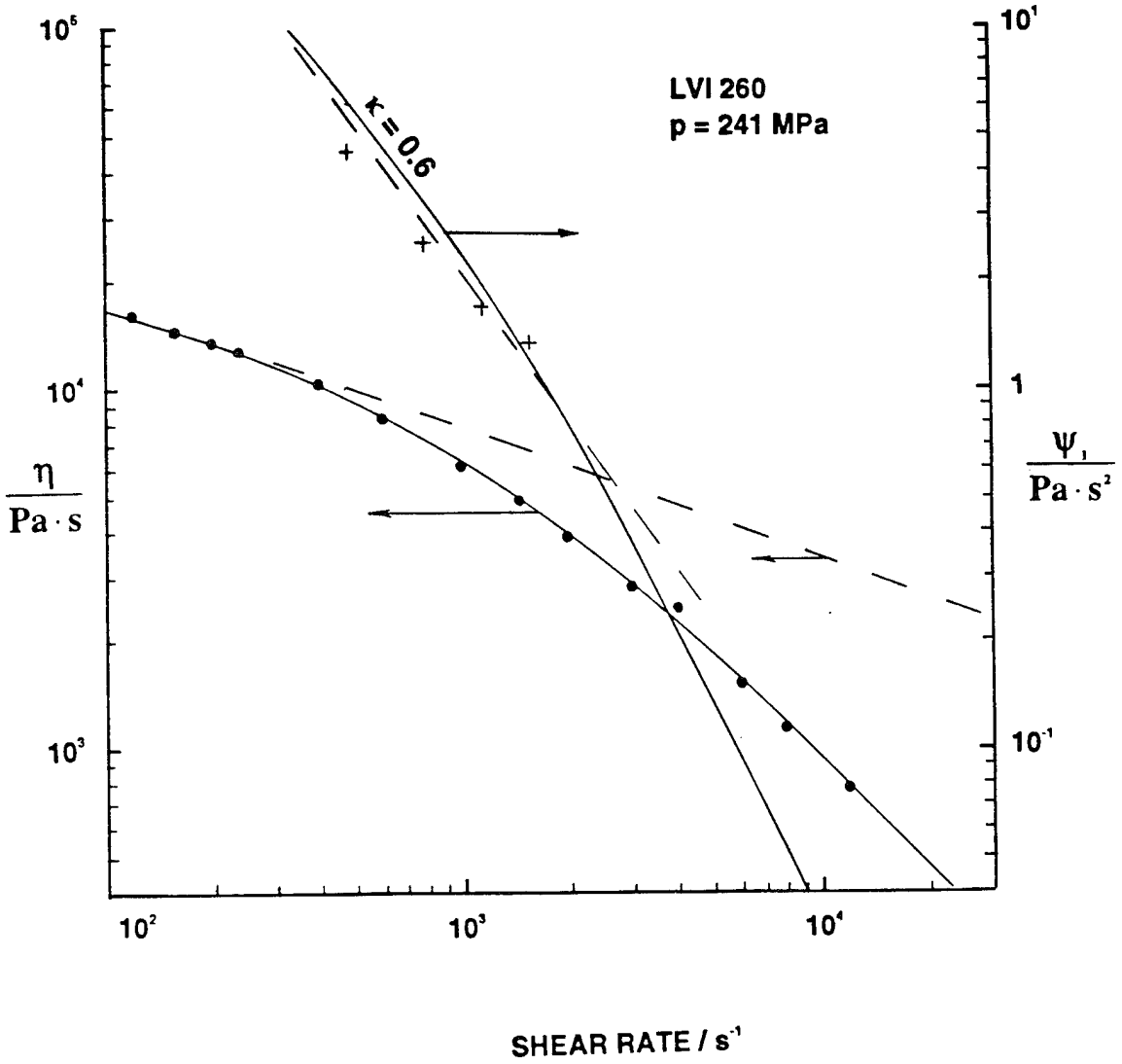

Figure 10. Viscosity and First Normal Stress Coefficient versus Shear Rate for LVI 260. The prediction of Equation (11) is plotted. ψ_1 - ψ_2 plotted as +.

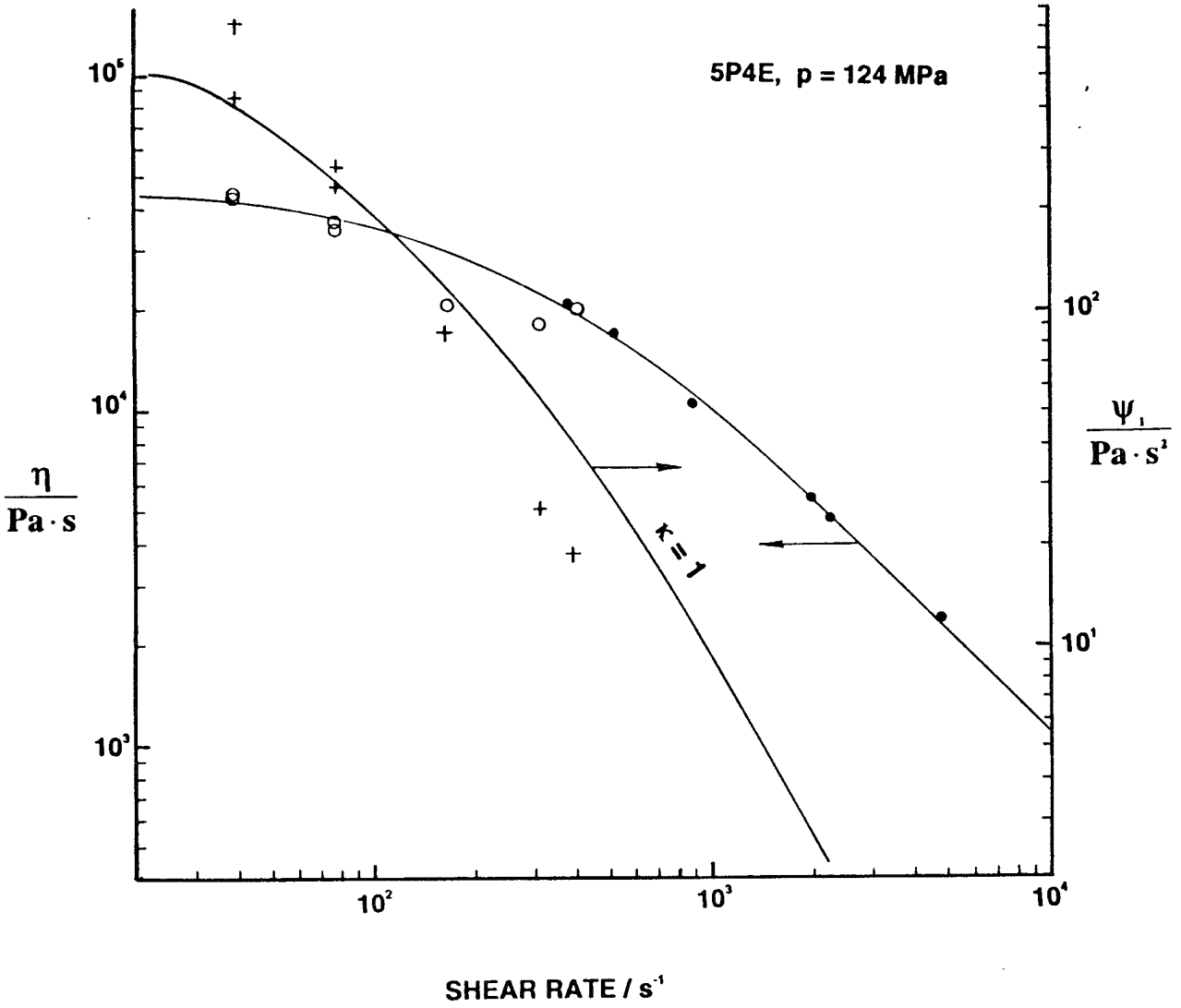

Figure 11. Viscosity and First Normal Stress Coefficient versus Shear Rate for 5P4E. The prediction of Equation (11) is plotted. ψ_1 - ψ_2 plotted as +.

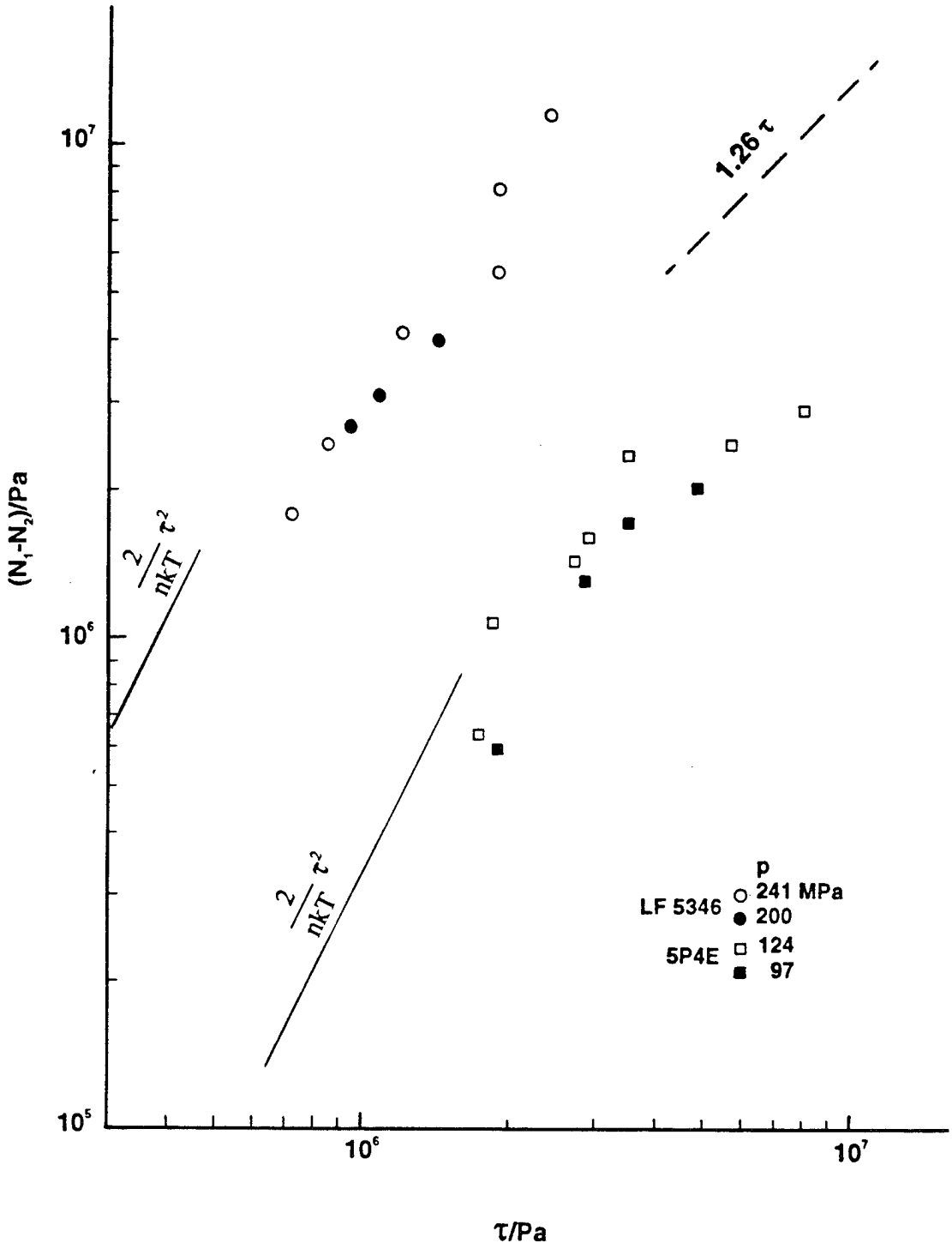

Figure 12. Normal Stress Difference versus Shear Stress Showing Effect of Pressure and Predictions.

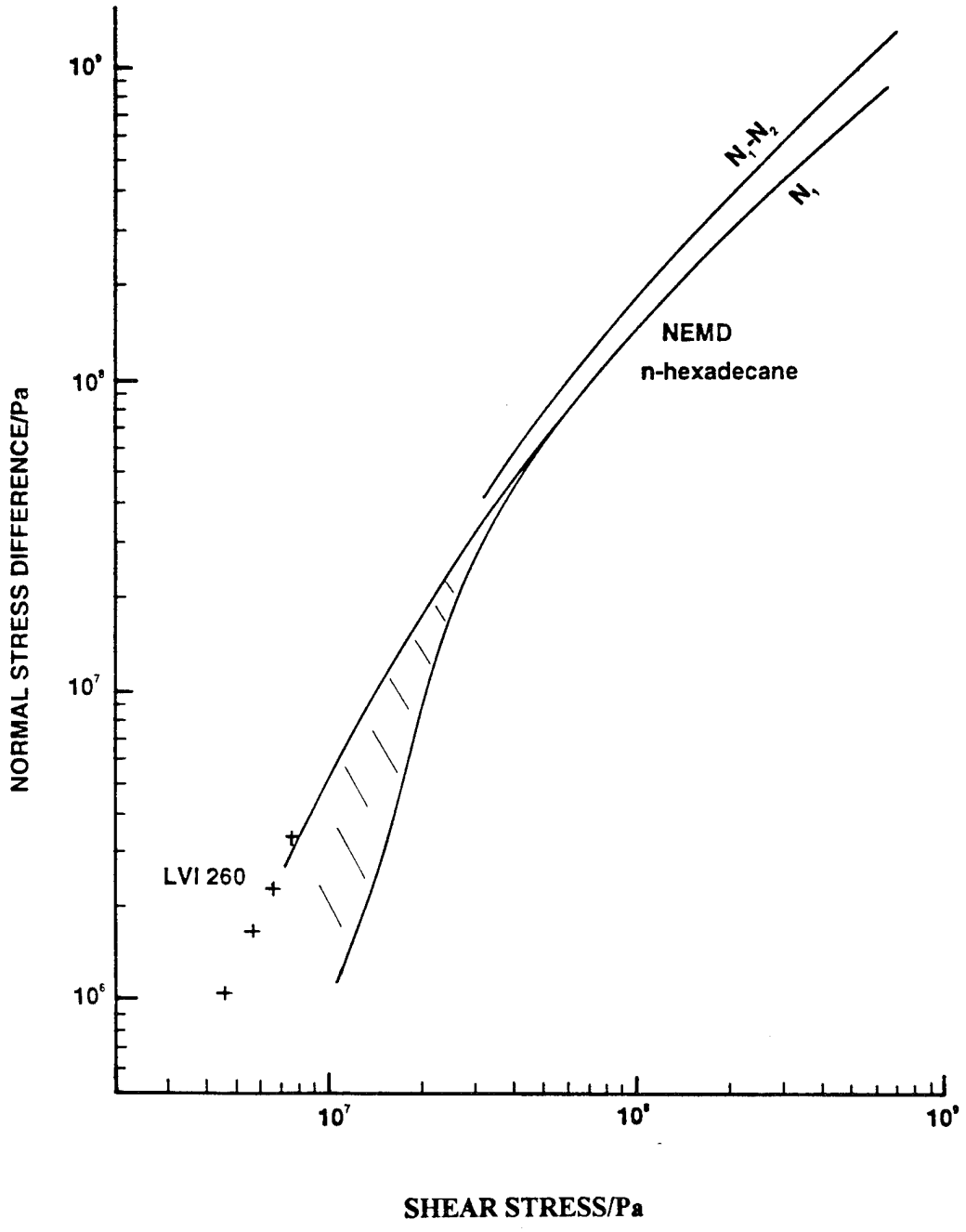

Figure 13. Comparison of Molecular Dynamic Simulation with Experimental Measurements.

Date: 8/20/95 Time: 6:59:39PM

Page: 1 Document Name: untitled

-- 1 OF 2
-- 1 - AD NUMBER: A288906
-- 2 - FIELDS AND GROUPS: 11/8
-- 5 - CORPORATE AUTHOR: GEORGIA INST OF TECH ATLANTA SCHOOL OF
-- MECHANICAL ENGINEERING
-- 6 - UNCLASSIFIED TITLE: DEFORMATION BEHAVIOR OF THIN LUBRICANT
-- FILMS AT ELEVATED PRESSURE.
--10 - PERSONAL AUTHORS: BAIR, SCOTT; QURESHI, F.; LEE, Y. K.; WINER, W. O.
--11 - REPORT DATE: DEC 1994
--12 - PAGINATION: 99P MEDIA COST: $ 6.00
--18 - MONITOR ACRONYM: XB
--19 - MONITOR SERIES: ONR
--20 - REPORT CLASSIFICATION: UNCLASSIFIED
--33 - LIMITATION CODES: 1